

Efficient Diels–Alder Addition of Cyclopentadiene to Lithium Ion Encapsulated [60]Fullerene

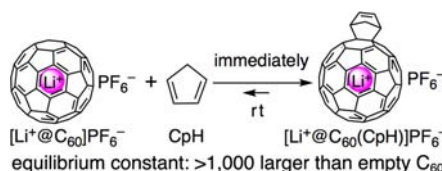
Hiroki Kawakami, Hiroshi Okada, and Yutaka Matsuo*

Department of Chemistry, School of Science, The University of Tokyo, 7-3-1 Hongo,
Bunkyo-ku, Tokyo 113-0033, Japan

matsuo@chem.s.u-tokyo.ac.jp

Received July 17, 2013

ABSTRACT



Much higher reactivity of $[\text{Li}^+@C_{60}]\text{PF}_6^-$ for Diels–Alder cycloaddition toward cyclopentadiene (CpH), in comparison with that of empty C_{60} , was observed. The synthetic method, electrochemical and light absorption properties, and X-ray crystal structure of the product $[\text{Li}^+@C_{60}(\text{CpH})]\text{PF}_6^-$ are discussed.

Lithium ion containing [60]fullerene, $\text{Li}^+@C_{60}$, was first isolated and structurally characterized in 2010.¹ Since being isolated in pure form, this emerging carbon nano-material has garnered interest in various areas of applied research.² To advance the investigation of $\text{Li}^+@C_{60}$, covalent modification of this compound should present new opportunities arising from changes in the compound's

electrochemical and photophysical properties. Such chemical modification of fullerenes generally plays a central role in developing fullerene-based materials,³ but few reports have focused on the chemical modification of $\text{Li}^+@C_{60}$.⁴ The present $\text{Li}^+@C_{60}$ covalent modification

(1) (a) Aoyagi, S.; Nishibori, E.; Sawa, H.; Sugimoto, K.; Takata, M.; Miyata, Y.; Litaura, R.; Shinohara, H.; Okada, H.; Sakai, T.; Ono, Y.; Kawachi, K.; Yokoo, K.; Ono, S.; Omote, K.; Kasama, Y.; Ishikawa, S.; Komuro, T.; Tobita, H. *Nat. Chem.* **2010**, *2*, 678–683. (b) Okada, H.; Komuro, T.; Sakai, T.; Matsuo, Y.; Ono, Y.; Omote, K.; Yokoo, K.; Kawachi, K.; Kasama, Y.; Ono, S.; Hatakeyama, R.; Kaneko, T.; Tobita, H. *RSC Adv.* **2012**, *2*, 10624–10631.

(2) (a) Fukuzumi, S.; Ohkubo, K.; Kawashima, Y.; Kim, D. S.; Park, J. S.; Jana, A.; Lynch, V. M.; Kim, D.; Sessler, J. L. *J. Am. Chem. Soc.* **2011**, *133*, 15938–15941. (b) Ohkubo, K.; Kawashima, Y.; Fukuzumi, S. *Chem. Commun.* **2012**, *48*, 4314–4316. (c) Ohkubo, K.; Kawashima, Y.; Sakai, H.; Hasobe, T.; Fukuzumi, S. *Chem. Commun.* **2013**, *49*, 4474–4476. (d) Kamimura, T.; Ohkubo, K.; Kawashima, Y.; Nobukuni, H.; Naruta, Y.; Tani, F.; Fukuzumi, S. *Chem. Sci.* **2013**, *4*, 1451–1461.

(3) (a) Takano, Y.; Herranz, M. A.; Martín, N.; Radhakrishnan, S. G.; Guldi, D. M.; Tsuchiya, T.; Nagase, S.; Akasaka, T. *J. Am. Chem. Soc.* **2010**, *132*, 8048–8055. (b) Feng, L.; Radhakrishnan, S. G.; Mizorogi, N.; Slanina, Z.; Nikawa, H.; Tsuchiya, T.; Akasaka, T.; Nagase, S.; Martín, N.; Guldi, D. M. *J. Am. Chem. Soc.* **2011**, *133*, 7608–7618. (c) Sato, S.; Seki, S.; Honsho, Y.; Wang, L.; Nikawa, H.; Luo, G.; Lu, J.; Haranaka, M.; Tsuchiya, T.; Nagase, S.; Akasaka, T. *J. Am. Chem. Soc.* **2011**, *133*, 2766–2771.

(4) (a) Matsuo, Y.; Okada, H.; Maruyama, M.; Sato, H.; Tobita, H.; Ono, Y.; Omote, K.; Kawachi, K.; Kasama, Y. *Org. Lett.* **2012**, *14*, 3784–3787. (b) Ueno, H.; Nakamura, Y.; Ikuma, N.; Kokubo, K.; Oshima, T. *Nano Res.* **2012**, *5*, 558–564.

(5) Wakahara, T.; Nikawa, H.; Kikuchi, T.; Nakahodo, T.; Rahman, G. M. A.; Tsuchiya, T.; Maeda, Y.; Akasaka, T.; Yoza, K.; Horn, E.; Yamamoto, K.; Mizorogi, N.; Slanina, Z.; Nagase, S. *J. Am. Chem. Soc.* **2006**, *128*, 14228–14229.

(6) Nikawa, H.; Kikuchi, T.; Wakahara, T.; Nakahodo, T.; Tsuchiya, T.; Rahman, G. M. A.; Akasaka, T.; Maeda, Y.; Yoza, K.; Horn, E.; Yamamoto, K.; Mizorogi, N.; Nagase, S. *J. Am. Chem. Soc.* **2005**, *127*, 9684–9685.

(7) (a) Cai, T.; Xu, L.; Gibson, H. W.; Dorn, H. C.; Chancellor, C. J.; Olmstead, M. M.; Balch, A. L. *J. Am. Chem. Soc.* **2007**, *129*, 10795–10800. (b) Cao, B.; Nikawa, H.; Nakahodo, T.; Tsuchiya, T.; Maeda, Y.; Akasaka, T.; Sawa, H.; Slanina, Z.; Mizorogi, N.; Nagase, S. *J. Am. Chem. Soc.* **2008**, *130*, 983–989.

(8) (a) Lee, H. M.; Olmstead, M. M.; Iezzi, E.; Duchamp, J. C.; Dorn, H. C.; Balch, A. L. *J. Am. Chem. Soc.* **2002**, *124*, 3494–3495. (b) Cai, T.; Ge, Z.; Iezzi, E. B.; Glass, T. E.; Harich, K.; Gibson, H. W.; Dorn, H. C. *Chem. Commun.* **2005**, 3594–3596. (c) Iiduka, Y.; Wakahara, T.; Nakahodo, T.; Tsuchiya, T.; Sakuraba, A.; Maeda, Y.; Akasaka, T.; Yoza, K.; Horn, E.; Kato, T.; Liu, M. T. H.; Mizorogi, N.; Nagase, S. *J. Am. Chem. Soc.* **2005**, *127*, 12500–12501.

(9) (a) Akasaka, T.; Kato, T.; Kobayashi, K.; Nagase, S.; Yamamoto, K.; Funasaka, H.; Takahashi, T. *Nature* **1995**, *374*, 600–601. (b) Maeda, Y.; Matsunaga, Y.; Wakahara, T.; Takahashi, S.; Tsuchiya, T.; Ishitsuka, M. O.; Hasegawa, T.; Akasaka, T.; Liu, M. T. H.; Kokura, K.; Horn, E.; Yoza, K.; Kato, T.; Okubo, S.; Kobayashi, K.; Nagase, S.; Yamamoto, K. *J. Am. Chem. Soc.* **2004**, *124*, 6858–6859. (c) Feng, L.; Nakahodo, T.; Wakahara, T.; Tsuchiya, T.; Maeda, Y.; Akasaka, T.; Kato, T.; Horn, E.; Yoza, K.; Mizorogi, N.; Nagase, S. *J. Am. Chem. Soc.* **2005**, *127*, 17136–17137.

represents a unique example, which can be distinguished from other endohedral metallofullerene modifications based on [72]-, [74]-, [78]-, [80]-, and [82]fullerene cages,^{5–9} as well as derivatization of molecular hydrogen encapsulated fullerenes.¹⁰

The Diels–Alder reaction is a typical reaction for chemical functionalization of fullerenes.¹¹ In general, the kinetics of the Diels–Alder reaction is more favorable when the energy difference is small between the highest occupied molecular orbital (HOMO) of the diene and the lowest unoccupied molecular orbital (LUMO) of the dienophile. In comparison with various olefins, fullerene has a lower-lying LUMO level and hence serves as a better dienophile. On the other hand, cyclopentadiene (CpH) and its derivatives have been used as dienes in Diels–Alder reactions with fullerenes. Since the first report of the Diels–Alder reaction between fullerene and CpH in 1993, this reaction has been examined through kinetics investigations and theoretical studies.¹² The Diels–Alder reaction of La@C₈₂ and cyclopentadienes has also been studied to elucidate the kinetics of the reaction and the crystal structure of the product.¹³ Because the LUMO level of Li⁺@C₆₀ is much lower than that of empty C₆₀ and also lower than that of La@C₈₂, the Diels–Alder reaction of Li⁺@C₆₀ is expected to proceed much more smoothly. In this respect, we focused on this relationship of frontier orbital energies and examined the Diels–Alder reaction of Li⁺@C₆₀ and CpH. This reaction occurred immediately, and we succeeded in isolating and structurally characterizing the CpH monoadduct of Li⁺@C₆₀. Here we report the highly efficient Diels–Alder addition of CpH to Li⁺@C₆₀ as well as the structure and properties of the covalently functionalized Li⁺@C₆₀ derivative. The present work will provide valuable information for derivatization of Li⁺@C₆₀ to obtain various functional endohedral fullerenes.

Reaction of [Li⁺@C₆₀]PF₆[−] in a mixed solvent of chlorobenzene and acetonitrile (1/1 volume ratio) with 1.1 equiv of CpH diluted in organic solvents (e.g., *o*-dichlorobenzene and dichloromethane) afforded the monoadduct [Li⁺@C₆₀(CpH)]PF₆[−] along with the regioisomers of bis-adducts [Li⁺@C₆₀(CpH)₂]PF₆[−] and unreacted

starting material [Li⁺@C₆₀]PF₆[−] (Scheme 1). The reaction progress was monitored with an analytical HPLC system equipped with an electrolyte (Bu₄NPF₆)-containing column (Figure S1, Supporting Information).¹⁴ Generation of mono- and bis-adducts was confirmed by mass and ⁷Li NMR spectra (Figures S2 and S3, Supporting Information). From the reaction mixture, the desired monoadduct [Li⁺@C₆₀(CpH)]PF₆[−] was isolated by preparative HPLC in 56% isolated yield. An HPLC chart of isolated [Li⁺@C₆₀(CpH)]PF₆[−] in pure form is shown in Figure S1c.¹⁵

Scheme 1. Reaction of [Li⁺@C₆₀]PF₆[−] with CpH



The isolated product was characterized by mass spectrometry, NMR spectroscopy, UV–vis absorption spectroscopy, and cyclic voltammetry. The high-resolution atmospheric pressure chemical ionization (APCI) time-of-flight (TOF) mass spectrum showed a single peak for [Li⁺@C₆₀(CpH)] at *m/z* 793.0661 (calcd 793.0631). The compound's ¹H NMR spectrum (Figure S5, Supporting Information) was similar to that of empty C₆₀(CpH), with only slight differences between them. The ¹³C NMR spectrum exhibited a C_s-symmetric pattern with 32 signals for the fullerene cage and 3 signals for CpH (Figure S6, Supporting Information). The ⁷Li NMR spectrum showed a high-field signal due to the lithium ion at high magnetic field (δ −13.4), indicating that the lithium ion is contained inside the fullerene cage (Figure S7, Supporting Information). The UV–vis absorption spectrum of [Li⁺@C₆₀(CpH)]PF₆[−] was very similar to that of empty C₆₀(CpH). The spectrum for [Li⁺@C₆₀(CpH)]PF₆[−] showed a small absorption maximum at 720 nm due to the 58- π -electron conjugated system of the fullerene cage (Figure S8, Supporting Information). The first reduction potential of [Li⁺@C₆₀(CpH)]PF₆[−] was −0.49 V vs Fc/Fc⁺. This value indicates that, in comparison with empty C₆₀-(CpH) (−1.22 V) and C₆₀ (−1.13 V), [Li⁺@C₆₀(CpH)]PF₆[−] has a much higher electron affinity (Table 1).

Next we performed a single-crystal X-ray structural analysis of [Li⁺@C₆₀(CpH)]. We first attempted X-ray crystallographic analysis of [Li⁺@C₆₀(CpH)]PF₆[−] but could not obtain a single crystal of sufficient quality. Then, we performed counteranion exchange, from PF₆[−] to tetrakis(3,5-bis(trifluoromethyl)phenyl)borate (TFPB[−]), by

(10) (a) Matsuo, Y.; Isobe, H.; Tanaka, T.; Murata, Y.; Murata, M.; Komatsu, K.; Nakamura, E. *J. Am. Chem. Soc.* **2005**, *127*, 17148–17149. (b) Murata, M.; Ochi, Y.; Kitagawa, T.; Komatsu, K.; Murata, Y. *Chem. Asian J.* **2008**, *3*, 1336–1342. (c) Li, Y.; Lawler, R. G.; Murata, Y.; Komatsu, K.; Turro, N. J. *J. Phys. Chem. Lett.* **2010**, *1*, 2135–2138.

(11) (a) Sarova, G. H.; Berberan-Santos, M. N. *Chem. Phys. Lett.* **2004**, *397*, 402–407. (b) Ohno, M.; Azuma, T.; Kojima, S.; Shirakawa, Y.; Eguchi, S. *Tetrahedron* **1996**, *52*, 4983–4994.

(12) (a) Pang, L. S. K.; Wilson, M. A. *J. Phys. Chem.* **1993**, *97*, 6761–6763. (b) Giovane, L. M.; Barco, J. W.; Yadav, T.; Lafleur, A. L.; Marr, J. A.; Howard, J. B.; Rotello, V. M. *J. Phys. Chem.* **1993**, *97*, 8560–8561.

(13) (a) Maeda, Y.; Miyashita, J.; Hasegawa, T.; Wakahara, T.; Tsuchiya, T.; Nakahodo, T.; Akasaka, T.; Mizorogi, N.; Kobayashi, K.; Nagase, S.; Kato, T.; Ban, N.; Nakajima, H.; Watanabe, Y. *J. Am. Chem. Soc.* **2005**, *127*, 12190–12191. (b) Ge, Z.; Duchamp, J. C.; Cai, T.; Gibson, H. W.; Dorn, H. C. *J. Am. Chem. Soc.* **2005**, *127*, 16292–16298. (c) Maeda, Y.; Sato, S.; Inada, K.; Nikawa, H.; Yamada, M.; Mizorogi, N.; Hasegawa, T.; Tsuchiya, T.; Akasaka, T.; Kato, T.; Slanina, Z.; Nagase, S. *Chem. Eur. J.* **2010**, *16*, 2193–2197. (d) Garcia-Borràs, M.; Luis, J. M.; Swart, M.; Solà, M. *Chem. Eur. J.* **2013**, *19*, 4468–4479. (e) Sato, S.; Maeda, Y.; Guo, J.-D.; Yamada, M.; Mizorogi, N.; Nagase, S.; Akasaka, T. *J. Am. Chem. Soc.* **2013**, *135*, 5582–5587.

(14) Analytical HPLC conditions: column, Buckyprep (Nacalai Tesque, COSMOSIL 4.6 × 250 nm); eluent, *o*-dichlorobenzene/acetonitrile 95/5 v/v with 30 mM Bu₄NPF₆; column temperature, 30 °C; detector, UV, 320 nm.

(15) Preparative HPLC conditions: column, π NAP (Nacalai Tesque, COSMOSIL 4.6 × 250 nm); eluent, chlorobenzene/*o*-dichloroethane/acetonitrile 2/1.5/6.5 v/v/v with saturated Me₄NPF₆; temperature, 30 °C.

Table 1. Reduction Potentials (V vs Fc/Fc⁺) for [Li⁺@C₆₀(CpH)]PF₆[−], [Li⁺@C₆₀]PF₆[−], C₆₀(CpH), and C₆₀^a

compd	$E_{1/2}^{\text{red1/V}}$	$E_{1/2}^{\text{red2/V}}$	$E_{1/2}^{\text{red3/V}}$	$E_{1/2}^{\text{red4/V}}$
[Li ⁺ @C ₆₀ (CpH)]PF ₆ [−]	−0.49	−1.05	−1.56	−1.93
[Li ⁺ @C ₆₀]PF ₆ [−]	−0.43	−1.02	−1.49	−1.90
C ₆₀ (CpH)	−1.22	−1.59	−2.11	
C ₆₀	−1.13	−1.51	−1.96	

^a Determined with cyclic voltammetry in *o*-dichlorobenzene containing 50 mM Bu₄NPF₆.

reacting [Li⁺@C₆₀(CpH)]PF₆[−] with NaTFPB (1.1 equiv) in dichloromethane. The product [Li⁺@C₆₀(CpH)]TFPB[−] was recrystallized by the vapor diffusion method using CH₂Cl₂/Et₂O. The obtained single crystal was subjected to X-ray crystallography to reveal the structure of the CpH adduct of Li⁺@C₆₀.¹⁶ The crystal structure (Figure 1) shows that the Diels–Alder addition of CpH occurred at the (6,6)-bond of the fullerene cage. This finding is in good agreement with the results of quantum mechanical studies on C₆₀(CpH), which showed that the (6,6)-adduct is more stable than the (5,6)-adduct.¹⁷ To date, X-ray crystallographic analysis of C₆₀(CpH) has yet to be performed. Crystallographic analysis of [Li⁺@C₆₀(CpH)]TFPB[−] was successful due to the low-lying LUMO of the dienophile, Li⁺@C₆₀, which imparts further electronic stability to the Diels–Alder product.

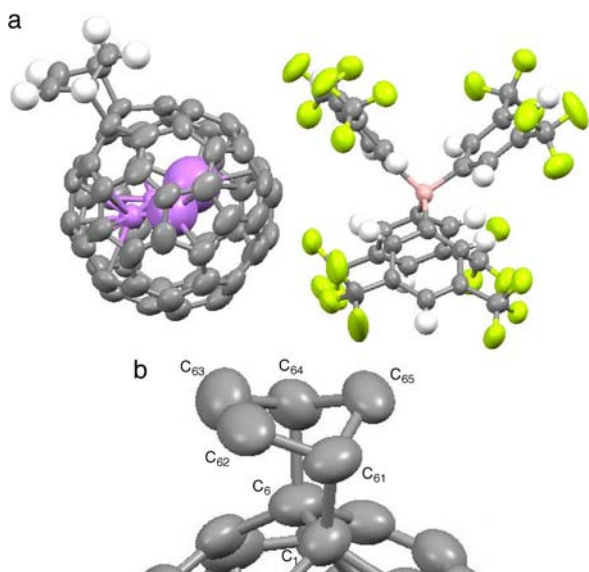


Figure 1. Crystal structure of [Li⁺@C₆₀(CpH)]TFPB[−]: (a) anion/cation pair in the crystal; (b) CpH moiety on the fullerene cage. Hydrogen atoms are omitted for clarity.

(16) CCDC No. 948210.

(17) (a) Osuna, S.; Moreta, J.; Cases, M.; Morokuma, K.; Solà, M. *J. Phys. Chem. A* **2009**, *113*, 9721–9726. (b) Fernández, I.; Solà, M.; Bickelhaupt, F. M. *Chem. Eur. J.* **2013**, *19*, 7416–7422.

A closer look at the crystallographic structure of [Li⁺@C₆₀(CpH)]TFPB[−] revealed the nature of the C–C bonds connecting Li⁺@C₆₀ and CpH as well as the dynamic behavior of the lithium atom inside the fullerene cage. Covalent bond lengths between C₆₀ and CpH (C₁–C₆₁ and C₆–C₆₄) were 1.594(7) and 1.636(8) Å, longer than for the length of a typical carbon–carbon single bond (1.54 Å). A similar structural feature has also been observed for the Diels–Alder adduct of La@C₈₂ with pentamethylcyclopentadiene (C₅Me₅H); C–C bond distances between carbon atoms of La@C₈₂ and C₅Me₅H have been reported to be 1.610 and 1.599 Å.¹³ We ascribed the long C–C bond distances between the fullerene cage and CpH to restricted degrees of freedom at the participating carbon atoms of the fullerene cage (C₁ and C₆) as well as at the CpH bridgehead carbon atoms (C₆₁ and C₆₄), which are constrained by the methylene group (C₆₅) and fullerene cage. These structural constraints partially weaken the newly formed C–C covalent bonds, making them longer. Regarding the position of the lithium ion, we observed a large thermal parameter for the lithium atom, which was isotropically optimized in the X-ray crystal structure analysis. This observation suggests partial delocalization of the lithium ion inside the fullerene cage. Such behavior of the lithium ion of Li⁺@C₆₀, even at low temperature, has been reported in the literature.¹⁸

Finally, we report details of the reactivity of Li⁺@C₆₀ as compared with Li⁺@C₆₀ and empty C₆₀. We performed time-course analysis for the reactions of [Li⁺@C₆₀]PF₆[−] and C₆₀ at the same concentration with 1.0 equiv of CpH (Figure 2). We observed that the reaction of Li⁺@C₆₀ with CpH reached equilibrium in 15 s. On the other hand, the reaction of C₆₀ with CpH proceeded slowly and achieved equilibrium after 40 min. The main product of the reaction using Li⁺@C₆₀ was the monoadduct [Li⁺@C₆₀(CpH)]PF₆[−], while that for C₆₀ was the unreacted starting material. These results indicate that both the rate constant (*k*) and the equilibrium constant (*K* > 1.6 × 10⁵ M^{−1}; see the Supporting Information) for Li⁺@C₆₀ are much larger than those for C₆₀ (*K*' ≈ 1.5 × 10² M^{−1}; see the Supporting Information). Our attempt to determine the rate constant *k* was unsuccessful because the reaction of Li⁺@C₆₀ was very fast.¹² Although our analysis was qualitative, its results will provide valuable information on controlling fullerene cage reactivity by encapsulation of inner ions.

We remark on the equilibrium constant of the Diels–Alder reaction. We consider that the present reaction offers an ideal system to estimate the electronic effect of the dienophiles on the equilibrium of the Diels–Alder reaction, because we can count out the steric effect of the dienophiles due to the similarity in size between C₆₀ and Li⁺@C₆₀. From the experimental results, we suggest that the low-lying LUMO level of Li⁺@C₆₀ not only accelerates the Diels–Alder reaction but also stabilizes the product. In other words, the lower LUMO level of the

(18) Aoyagi, S.; Sado, Y.; Nishibori, E.; Sawa, H.; Okada, H.; Tobita, H.; Kasama, Y.; Kitaura, R.; Shinohara, H. *Angew. Chem., Int. Ed.* **2012**, *51*, 3377–3381.

dienophiles was responsible for the increase in both the rate constant and the equilibrium constant.

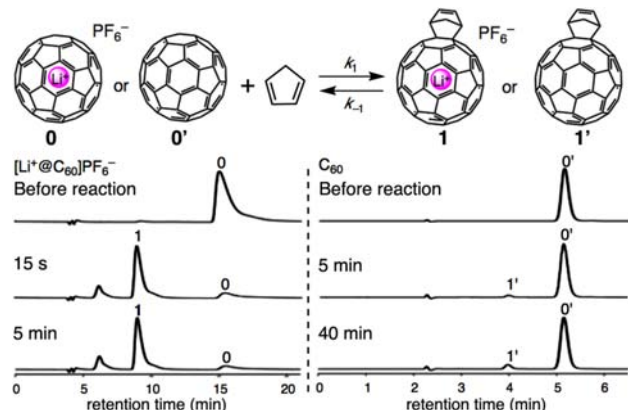


Figure 2. Comparison of reactivity of $[\text{Li}^+@C_{60}]\text{PF}_6^-$ and C_{60} toward CpH.

In summary, we have demonstrated the Diels–Alder addition of CpH to $\text{Li}^+@C_{60}$ and found that this reaction was highly efficient, with an equilibrium constant that was more than 10^3 -fold that for the reaction with empty C_{60} . This result clearly reveals the effect of the encapsulated

lithium ion on the reactivity of the fullerene cage. In addition, we have reported the X-ray crystal structure and properties of the Diels–Alder product. These findings and data should provide useful hints for covalently modifying endohedral fullerene $\text{Li}^+@C_{60}$, which is an emerging material in applied research.

Acknowledgment. This research was supported by the Japan Society for the Promotion of Science (JSPS) through the Funding Program for Next Generation World-Leading Researchers (NEXT) Program, initiated by the Council for Science and Technology Policy (CSTP). The ^{13}C NMR measurements were supported by the “Nanotechnology Platform” of the Ministry of Education, Culture, Sports, Science and Technology (MEXT) of Japan, at the Center for Integrated Nanotechnology Support, Tohoku University.

Supporting Information Available. Text, figures, and a table giving synthesis and characterization data, analytical HPLC charts, APCI-TOF mass spectra, ^1H and ^7Li NMR spectra, UV–vis spectra, cyclic voltammograms, X-ray crystal structure data and details of experiments, and estimation of equilibrium constants. This material is available free of charge via the Internet at <http://pubs.acs.org>.

The authors declare no competing financial interest.